

Short Paper

A speleothem record of Younger Dryas cooling, Klamath Mountains, Oregon, USA

David A. Vacco^{a,*}, Peter U. Clark^b, Alan C. Mix^c, Hai Cheng^d, R. Lawrence Edwards^d

^aDepartment of Geosciences, Pennsylvania State University, State College, PA 16802, USA

^bDepartment of Geosciences, Oregon State University, Corvallis, OR 97331, USA

^cCollege of Oceanic and Atmospheric Sciences, Oregon State University, Corvallis, OR 97331, USA

^dDepartment of Geology and Geophysics, University of Minnesota, Minneapolis, MN 55455, USA

Received 9 November 2004

Available online 20 July 2005

Abstract

A well-dated $\delta^{18}\text{O}$ record in a stalagmite from a cave in the Klamath Mountains, Oregon, with a sampling interval of 50 yr, indicates that the climate of this region cooled essentially synchronously with Younger Dryas climate change elsewhere in the Northern Hemisphere. The $\delta^{18}\text{O}$ record also indicates significant century-scale temperature variability during the early Holocene. The $\delta^{13}\text{C}$ record suggests increasing biomass over the cave through the last deglaciation, with century-scale variability but with little detectable response of vegetation to Younger Dryas cooling.

© 2005 University of Washington. All rights reserved.

Keywords: Stalagmite; Younger Dryas; Klamath Mountains

Introduction

Climate records spanning the last deglaciation reveal several large and abrupt climate changes that may have been hemispheric or perhaps global in extent (Clark et al., 2002; Voelker et al., 2002). The mechanisms responsible for these events remain uncertain, but understanding their full spatial extent will provide insight into their origin, which represents an important objective because of the possible recurrence of analogous events in the future (Alley et al., 2003).

One strategy toward constraining potential mechanisms of abrupt climate change is to develop well-dated climate records with the temporal precision necessary to establish the regional amplitude and phasing of changes in the various components of the climate system. Many terrestrial records are of too low resolution, however, to identify abrupt climate changes. Moreover, the chronology of most climate

records of the last deglaciation is based on radiocarbon, thus preventing firm correlations among records because of uncertainties in local reservoir ages and corrections for changing ^{14}C production rate as they propagate through the carbon cycle.

Speleothems circumvent many of these issues by providing high-resolution climate records with chronologies anchored by precise U-Th ages. Here, we develop a precisely dated isotope record ($\delta^{18}\text{O}$, $\delta^{13}\text{C}$) of the last deglaciation from a stalagmite recovered from the Klamath Mountains, southwestern Oregon (Fig. 1). Since the climate of the region is strongly influenced by the Pacific Ocean, this record is significant in providing one of the few precisely dated terrestrial records of Northeast Pacific climate variability during the last deglaciation.

Setting

The Oregon Caves National Monument (OCNM) is located 65 km inland of the Pacific coast of Oregon

* Corresponding author.

E-mail address: dvacco@geosc.psu.edu (D.A. Vacco).

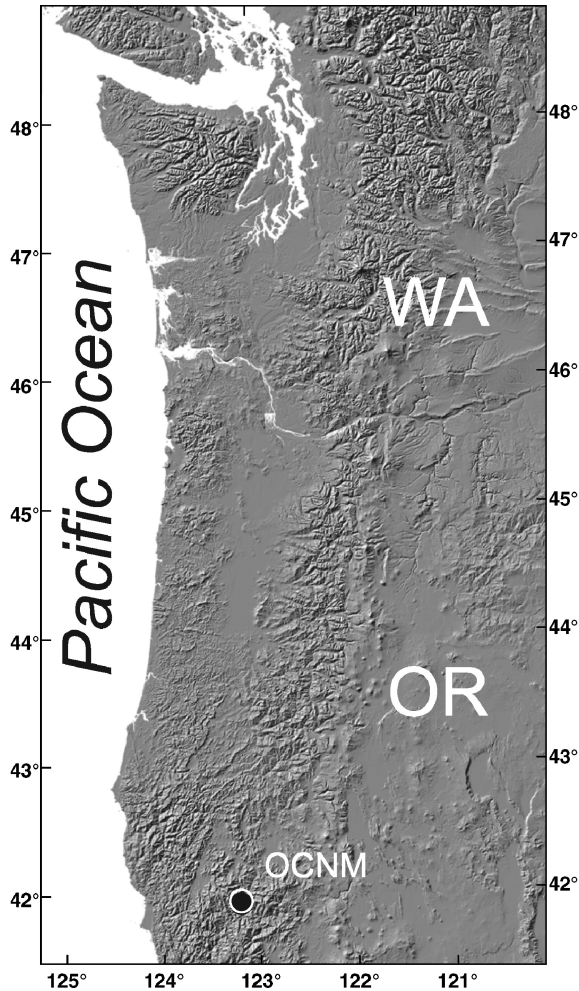


Figure 1. Location of Oregon Caves National Monument (42°05'N, 123°25'W) in southwestern Oregon.

(42°05'N, 123°25'W) (Fig. 1) at an elevation of ~1100 m above sea level. The cave system is developed in Triassic marble underlying the Klamath Mountains. The present-day cave air temperature averages about 7°C, varying only within narrow limits on a seasonal basis (Turgeon, 2001). The cave system reaches a depth of approximately 60 m below its main opening, and groundwater flows into the cave through the carbonate bedrock. Our sample was removed from the cave in the 1930s and was loaned to Oregon State University in 2000 for analysis.

Methods

We cut the OCNM stalagmite in half, parallel to the growth direction (Fig. 2). The polished stalagmite appears pristine, with no visible indication of post-depositional recrystallization. Calcite powder was milled for stable isotope measurements using a 350- μ m drill bit, yielding ~100 μ g of calcite. Oxygen and carbon isotope ratios were measured at Oregon State University using a Finnigan MAT 252 mass spectrometer and a Kiel-III online acid digestion

system. Average internal precision on carbonate analyses was $\pm 0.02\text{‰}$ and $\pm 0.01\text{‰}$ on $\delta^{18}\text{O}$ and $\delta^{13}\text{C}$, respectively. External precision of replicate analyses of a local carbonate standard (Wiley marble) run daily on this system, in the same size range as the speleothem samples and over the same time interval, was $\pm 0.06\text{‰}$ for $\delta^{18}\text{O}$ and $\pm 0.02\text{‰}$ for $\delta^{13}\text{C}$ (± 1 standard deviation, $n = 722$). Calibration to the widely used Vienna Pee Dee Belemnite (VPDB) standard was done via certified carbonate standards provided by the US National Institute of Standards and Technology (NIST). During the analysis period, the isotopic values and precision we obtained for NIST-8543 (also known as NBS-18 carbonatite) were $-23.02 \pm 0.11\text{‰}$ for $\delta^{18}\text{O}$ and $-5.04 \pm 0.04\text{‰}$ for $\delta^{13}\text{C}$ ($n = 23$), which compares with certified values of $-23.05 \pm 0.19\text{‰}$ and $-5.04 \pm 0.06\text{‰}$ for $\delta^{18}\text{O}$ and $\delta^{13}\text{C}$, respectively (NIST, 1992a). The isotopic values and precision we obtained for NIST-8544 (also known and NBS-19 limestone) were $-2.19 \pm 0.06\text{‰}$ for $\delta^{18}\text{O}$ and



Figure 2. Photograph of OCNM stalagmite, parallel to the growth direction. Black ovals are centered at sites sampled for U-Th dating. Scale bar (length of stalagmite) is 26.5 cm.

Table 1
 ^{230}Th dating results on OCNM stalagmite

Sample number	Sample depth (mm) (from base)	^{238}U (ppb)	^{232}Th (ppt)	$\delta^{234}\text{U}^*$ (measured)	$^{230}\text{Th}/^{238}\text{U}$ (activity)	^{230}Th age (years) (uncorrected)	^{230}Th age (years) (corrected)	$\delta^{234}\text{U}$ initial** (corrected)
A4	196	115.0 ± 0.2	154 ± 20	89.1 ± 3.3	0.0584 ± 0.0015	6010 ± 160	5914 ± 160	90.6 ± 3.3
A7	158	134.2 ± 0.2	630 ± 13	102.5 ± 2.1	0.0965 ± 0.0011	9980 ± 130	9650 ± 140	105.3 ± 2.1
A9	147	126.9 ± 0.3	475 ± 12	111.9 ± 3.7	0.1062 ± 0.0015	10,950 ± 170	10,680 ± 170	115.3 ± 3.8
A12	147	127.6 ± 0.1	878 ± 12	110.4 ± 1.8	0.1096 ± 0.0010	11,330 ± 110	10,840 ± 150	113.8 ± 1.8
A13	147	126.1 ± 0.1	1832 ± 13	105.4 ± 1.8	0.1146 ± 0.0010	11,930 ± 120	10,880 ± 250	108.7 ± 1.8
A8	134	159.2 ± 0.3	2308 ± 13	129.4 ± 2.1	0.1224 ± 0.0011	12,500 ± 120	11,480 ± 240	133.7 ± 2.1
A10	134	164.8 ± 0.2	2590 ± 12	122.0 ± 1.5	0.1251 ± 0.0010	12,880 ± 110	11,770 ± 260	126.1 ± 1.6
A11	134	151.1 ± 0.2	2450 ± 17	99.0 ± 2.0	0.1237 ± 0.0013	13,020 ± 150	11,840 ± 290	102.4 ± 2.1
A6	129	103.1 ± 0.2	1317 ± 12	134.0 ± 3.0	0.1262 ± 0.0014	12,850 ± 160	11,960 ± 240	138.6 ± 3.2
A3	119	170.9 ± 0.3	433 ± 20	107.6 ± 2.5	0.1271 ± 0.0016	13,280 ± 170	13,100 ± 180	111.7 ± 2.6
A5	107	95.3 ± 0.1	2904 ± 16	109.4 ± 3.0	0.4778 ± 0.0031	60,860 ± 570	58,700 ± 720	129.1 ± 3.5
A2	96	208.8 ± 0.3	190 ± 20	89.4 ± 2.5	0.7381 ± 0.0041	120,750 ± 1330	120,690 ± 1330	125.7 ± 3.6
A1	23	81.0 ± 0.2	255 ± 20	130.7 ± 6.9	0.8060 ± 0.0062	131,230 ± 2600	131,020 ± 2600	189 ± 10

$\lambda_{230} = 9.1577 \times 10^{-6} \text{ y}^{-1}$, $\lambda_{234} = 2.8263 \times 10^{-6} \text{ y}^{-1}$, $\lambda_{238} = 1.55125 \times 10^{-10} \text{ y}^{-1}$. * $\delta^{234}\text{U} = ([^{234}\text{U}/^{238}\text{U}]_{\text{activity}} - 1) \times 1000$. ** $\delta^{234}\text{U}_{\text{initial}}$ was calculated based on ^{230}Th age (T), i.e., $\delta^{234}\text{U}_{\text{initial}} = \delta^{234}\text{U}_{\text{measured}} \times e^{234\lambda T}$. Corrected ^{230}Th ages assume the initial $^{230}\text{Th}/^{232}\text{Th}$ atomic ratio of $12.0 \pm 2.5 \times 10^{-6}$ based on three-point isochron (A9, A12 and A13), without U corrections. The error is 2σ error. Samples A8, A10 and A11 are from the same stalagmite growth layer, as are samples A9, A12 and A13.

+1.94 ± 0.02‰ for $\delta^{13}\text{C}$ ($n = 25$), which compares with certified values of −2.20‰ and +1.95‰ for $\delta^{18}\text{O}$ and $\delta^{13}\text{C}$, respectively (no precision estimate; NIST, 1992). As an additional check on isotopic calibration, we continue to run the traditional standard NBS-20 (Solenhofen limestone), although it is no longer accepted by NIST as a certified standard due to heterogeneity. For this unofficial standard we measured isotopic values and precision of −4.13 ± 0.06‰ for $\delta^{18}\text{O}$ and −1.05 ± 0.02‰ for $\delta^{13}\text{C}$ ($n = 19$), which compares well with the traditional values of −4.14‰ and −1.06‰ that are commonly used in the literature.

Oxygen isotope analyses of cave dripwaters used standard $\text{H}_2\text{O}/\text{CO}_2$ equilibration methods (Epstein and Mayeda, 1953), using a Finnigan/MAT 251 mass spectrometer at Oregon State University equipped with an automated equilibrator of local design. The isotopic composition of waters is reported relative to VSMOW based on analyses of the standards NIST-8535 (VSMOW), NIST-8536 (GISP, −24.85‰) and 8537 (SLAP, −55.5‰) (NIST, 1992b). The reproducibility of local reference waters is routinely ±0.04‰ on this system.

Approximately 200 mg of calcite powder was milled for U-Th dating using a 2-mm drill bit. Milling troughs were ~2.5 mm wide in the growth direction, 2 mm deep and 20–25 mm long following visible growth bands (roughly perpendicular to stalagmite growth direction). We obtained thirteen U-Th ages on powdered calcite using sector inductively coupled mass spectrometry at the University of Minnesota (Table 1). Methods are modifications of those presented in Edwards et al. (1987) and are described in Cheng et al. (2000) and Shen et al. (2002). Based on three coeval samples (A9, A12 and A13) (Table 1), we used the isochron technique (see Dorale et al., 2004) to calculate the initial $^{230}\text{Th}/^{232}\text{Th}$, which was 12.0 ± 2.5 ppm. For samples of about Younger Dryas age, the error in age, including the ±2.5

ppm error in initial thorium isotopic composition and the analytical error, is about ±200 years. Most of this error comes from the uncertainty in our knowledge of initial thorium isotopic composition. Replicate analyses show excellent reproducibility, and the U-Th ages are in stratigraphic order (Table 1), indicating that the $^{234}\text{U}/^{230}\text{Th}$ isotopic system has remained closed since calcite deposition.

Age model

Dating of speleothems from OCNM indicates that growth phases occurred primarily during terminations and interglacial

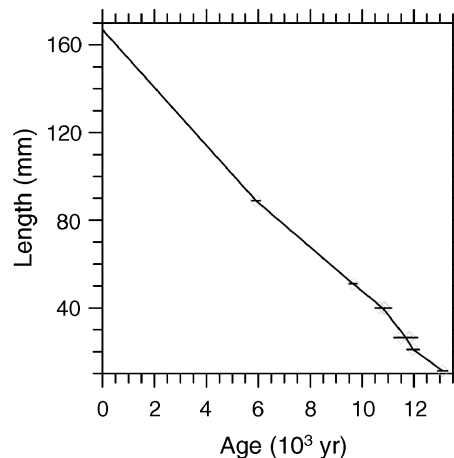


Figure 3. Age model for section of OCNM stalagmite <13,100 yr old, based on ten U-Th ages and assumption that top of stalagmite corresponds to year 0. Age model is constructed by linear interpolation between U-Th ages. For those two intervals where three U-Th ages were obtained, the age model is fitted to the error-weighted mean of the three ages from each interval.

ciations (Table 1) (Turgeon, 2001). The U-Th ages from our studied stalagmite reveal that deposition occurred primarily during two periods: ~ 131 to 120×10^3 yr ago, and since 13,300 yr ago, with a brief interval of deposition $\sim 59,000$ yr ago (Table 1). We constructed an age model for the last 13,300 yr using ten U-Th ages and assuming that the top of the stalagmite corresponds to year 0 (the stalagmite was collected in the 1930s) (Fig. 3). We focused our isotopic measurements on the best-dated interval (constrained by nine ages, including two intervals with three replicates each) between 13,300 yr ago and 9200 yr ago. During most of this time, calcite deposition rates ranged from $0.85 \text{ mm } 100 \text{ yr}^{-1}$ to $1.5 \text{ mm } 100 \text{ yr}^{-1}$, with a brief interval of $2 \text{ mm } 100 \text{ yr}^{-1}$ (Fig. 3). Consequently, the number of years averaged in most samples for dating (2.5 mm in growth direction) is similar to the U-Th uncertainty (180–360 yr). We define our age model for stable isotope values by linear interpolation between dated intervals. Based on this age model, our stable isotope samples (nominally 400- μm holes) average variations over 30–60 years, with an average sample spacing corresponding to ~ 50 yr.

Results

We ran a Hendy test (Hendy, 1971) to assess the absence of non-equilibrium effects, evaporative effects or effects resulting from prior calcite deposition during formation of speleothem calcite, recognizing that the potential for sampling multiple laminae may lead to large uncertainties. Based on five stable isotope measurements from a single growth ring, the linear regression skill for correlation between $\delta^{13}\text{C}$ and $\delta^{18}\text{O}$ was $R^2 = 0.58$, well below the 95% significance critical value of $R_{\text{crit}}^2 = 0.96$, suggesting that our sample was not subject to significant effects of this sort. A previous study of OCNM speleothems found similar results (Turgeon, 2001).

An additional evaluation of evaporative effects is based on the fact that speleothems deposited under isotopic equilibrium should have constant $\delta^{18}\text{O}$ of calcite ($\delta^{18}\text{O}_c$) values along a single growth band, owing to the relatively large amount of water available (Fantidis and Ehhalt, 1970; Hendy, 1971). We tested our sampling strategy for stable isotopes on this assumption by drilling at varying distances perpendicular to the growth axis. Isotopic measurements along the growth axis show no significant correlation between $\delta^{18}\text{O}_c$ and sample distance from the growth axis, thus further suggesting deposition under isotopic equilibrium.

Variations in $\delta^{18}\text{O}$ of stalagmite calcite reflect the temperature dependence of calcite-water isotopic fractionation and the $\delta^{18}\text{O}$ of cave dripwaters. The equilibrium fractionation in the calcite-water relationship is $-0.24\text{‰ } ^\circ\text{C}^{-1}$ (O'Neill et al., 1969). Observations from mid- to high latitudes (Dansgaard, 1964; Rozanski et al., 1993) suggest that $\delta^{18}\text{O}$ in precipitation ($\delta^{18}\text{O}_p$) has a temperature

dependence of $0.5\text{--}0.7\text{‰ } ^\circ\text{C}^{-1}$ (relative to surface air temperature). Four dripwater samples were collected from OCNM, and compared to the mean surface air temperature of the previous month, indicating an approximate temperature dependence of $0.46\text{‰ } ^\circ\text{C}^{-1}$. Although additional sampling from OCNM is required to quantify this site-specific relationship, these preliminary data indicate that $\delta^{18}\text{O}_c$ variations at OCNM are currently a function of air temperature. We qualitatively interpret changes in $\delta^{18}\text{O}_c$ to be positively correlated to surface temperature changes. In addition to temperature, several other factors may cause temporal variations in $\delta^{18}\text{O}_p$. Given the location of our site within 60 km of the Pacific Ocean, we focus on two potential effects: changing seawater composition and changes in moisture sources. We accounted for the effect of changing seawater $\delta^{18}\text{O}$ ($\delta^{18}\text{O}_{\text{sw}}$) by assigning a modern $\delta^{18}\text{O}_{\text{sw}}$ value of 0‰ and a last glacial maximum (LGM) value for the Pacific Ocean of 1‰ (Adkins et al., 2002). We then used the record of deglacial sea-level rise (Fleming et al., 1998) to interpolate $\delta^{18}\text{O}_{\text{sw}}$ values between the LGM and present and subtracted this signal from our measured $\delta^{18}\text{O}_c$ record.

It is more difficult to constrain the potential effect of changing moisture sources on our record, but examination of controls on modern climatology provides some insights into this question. We note that the current primary moisture source for the Pacific Northwest is derived from the central North Pacific associated with seasonal (winter) intensification of the Aleutian low-pressure cell. Source waters in this region are relatively isotopically homogenous (Schmidt et al., 1999), and any significant change in the $\delta^{18}\text{O}$ of moisture would require a significant southward shift to a subtropical Pacific source, implicating a major reorganization of controls on atmospheric circulation over the Pacific Ocean.

We have no evidence that such reorganizations have occurred at the time scales of relevance to our record. For example, Ortiz et al. (1997) reconstructed flow of the northern California Current during the Last Glacial Maximum, and argued for relatively small changes in the position of the subpolar front, and continued presence of a subtropical gyre system off southern Oregon. Given this modest change to the extremes of the Last Glacial Maximum, we expect that plausible long-term atmospheric changes were of a magnitude similar to those that occur on a seasonal basis (changes in ocean–continent heating and attendant changes in the strength of the Aleutian low-pressure cell). Mantua et al. (1997) formulated the Pacific Decadal Oscillation (PDO) index, whereby a positive (negative) index is associated with cooler (warmer) SSTs in the central North Pacific, and warmer (cooler) SSTs in the Gulf of Alaska and along the Pacific coast of North America. The PDO parallels the dominant pattern of North Pacific sea-level pressure (SLP) variability, such that cooler than average SSTs occur during periods of lower than average SLP over the central North Pacific and vice

versa. Although coupled ocean–atmosphere general circulation models (GCMs) are of relatively coarse resolution, available simulations of millennial-scale changes that may have affected the Pacific Ocean based on such models suggest that the largest response was in sea-surface temperatures over the North Pacific, which was associated with intensification but not a major shift in the position of the westerlies near 50°N (Mikolajewicz et al., 1997). Atmospheric GCM simulations suggest that the primary response to orbital-scale changes and other large-scale boundary conditions that occurred during the last deglaciation involved a strengthening of the Aleutian low-pressure cell with only minor shifts in the storm tracks in our region (Bartlein et al., 1998).

The $\delta^{13}\text{C}$ value in a speleothem reflects some combination of the $\delta^{13}\text{C}$ of the overlying soil zone, the $\delta^{13}\text{C}$ of the underlying bedrock and the processes involved in calcite precipitation (Hendy, 1971). With continuous equilibration between the soil water and an unlimited soil CO_2 reservoir, the $\delta^{13}\text{C}$ value of the dissolved inorganic carbon (DIC) is determined by the $\delta^{13}\text{C}$ value of soil CO_2 , which in turn depends on the ratio of C_3 plants ($\delta^{13}\text{C} \sim -26\text{‰}$) to C_4 plants ($\delta^{13}\text{C} \sim -13\text{‰}$) living in the soil, and on the ratio of atmospheric CO_2 ($\delta^{13}\text{C} = -7\text{‰}$) to biogenic CO_2 in the soil system (Cerling, 1984; Cerling et al., 1989; Genty et al., 2003). Dissolution of carbonate rock below the soil increases the $\delta^{13}\text{C}$ of DIC when the percolating water becomes isolated from the soil CO_2 reservoir. Further increases in $\delta^{13}\text{C}$ values may occur by CO_2 degassing of percolating waters and resulting calcite mineralization in the aquifer above the cave, rapid degassing of dripwaters in the cave, evaporation and kinetic fractionation (Baker et al., 1997).

Discussion

The last interglacial growth phase dated within the speleothem dated here agrees within error with a wet monsoon interval recorded in a speleothem record from Dongge Cave, China (Yuan et al., 2004). The growth phase dated in subsample A5 ($58.7 \pm 0.7 \times 10^3$ yr) correlates with a wet monsoon interval in Hulu Cave, China, (Wang et al., 2001) and with interstadial 17 from the GISP2 ice core, Greenland.

The next major growth phase began $\sim 13,300$ yr ago and continued to the present (Fig. 3). Following the removal of secular changes in $\delta^{18}\text{O}_{\text{sw}}$, OCNM $\delta^{18}\text{O}$ values range from -9.0 to -10.6‰ between 13,300 and 9200 yr ago (Fig. 4c). For comparison, an actively forming stalactite in OCNM has a $\delta^{18}\text{O}$ value of -8.7‰ (Turgeon, 2001). The most pronounced signal is a change to lower (more negative) $\delta^{18}\text{O}$ values that, within dating uncertainties, is synchronous with the onset of the Younger Dryas (YD) interval as defined by precisely dated, high-resolution isotope records from the GISP2 ice core (Fig. 4a) (Stuiver and Grootes,

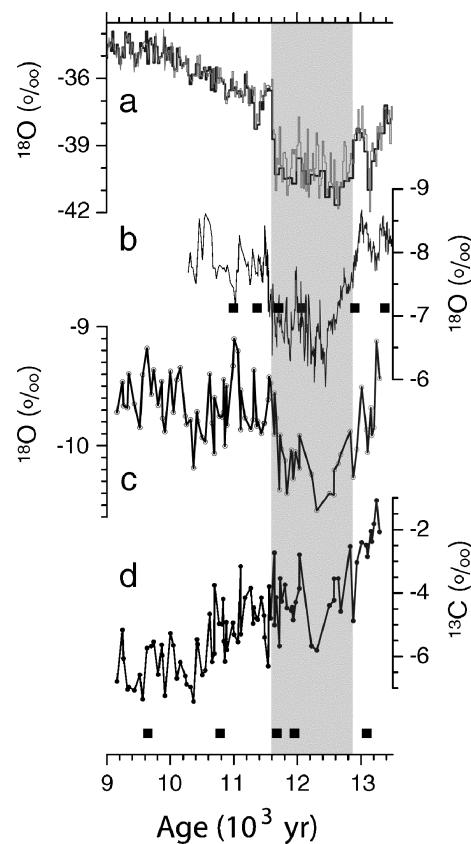


Figure 4. (a) Greenland GISP2 $\delta^{18}\text{O}$ record (Grootes et al., 1993; Stuiver and Grootes, 2000). (b) $\delta^{18}\text{O}$ record from Hulu Cave, China (Wang et al., 2001). (c) $\delta^{18}\text{O}$ record from OCNM. (d) $\delta^{13}\text{C}$ record from OCNM. U-Th age control is indicated by black squares (with 2σ error bars) at the bottom. The U-Th ages at $10,790 \pm 100$ yr and $11,680 \pm 150$ yr are the error-weighted mean ages of three coeval samples (Table 1).

2000) and a stalagmite from Hulu Cave, China (Fig. 4b) (Wang et al., 2001; Yuan et al., 2004). Specifically, OCNM $\delta^{18}\text{O}$ values begin a gradual decrease at $12,840 \pm 200$ yr ago, in excellent agreement with the timing of the onset of the YD at GISP2 ($12,880 \pm 260$ yr ago) and Hulu Cave ($12,823 \pm 60$ yr ago). Unlike the abrupt onset of the YD in the GISP2 record, however, our record is more similar to that from Hulu Cave in showing a gradual change in $\delta^{18}\text{O}$ values, culminating with the most extreme values at $\sim 12,300$ yr ago at OCNM and $\sim 12,400$ yr ago at Hulu Cave. Subsequently, both stalagmite records suggest an oscillation in $\delta^{18}\text{O}$ during the YD. Finally, the OCNM record registers an abrupt increase in $\delta^{18}\text{O}$ values at $11,700 \pm 260$ yr ago (uncertainty based on U-Th dates) that is synchronous with the abrupt termination of the YD in GISP2 ($11,640 \pm 250$ yr ago) and in Hulu Cave ($11,550 \pm 100$ yr ago) (Fig. 4).

The YD interval in OCNM $\delta^{18}\text{O}$ corresponds to a change of 0.75‰ . Insofar as the dominant control on $\delta^{18}\text{O}_c$ in our OCNM stalagmite is atmospheric temperature, a 0.75‰ change corresponds to cooling over the cave during the YD interval. This cooling is in qualitative agreement with

the $>3^{\circ}\text{C}$ YD cooling of sea-surface temperatures (SSTs) recorded in marine core ODP-1019 120 km due west of OCNM based on foraminifera (Mix et al., 1999) and an organic alkenone index (Barron et al., 2003). SST records to the north (Kienast and McKay, 2001) and south (Mortyn et al., 1996) of the Oregon margin confirm that cooling of the northeast Pacific was widespread during the YD.

From the termination of YD cooling until 9200 yr ago (the end of our record), $\delta^{18}\text{O}$ values range from -10.2 and -9.1‰ , averaging -9.8‰ (Fig. 4c). A 5-cm stalagmite from OCNM that grew between 4000 and 2000 yr ago has $\delta^{18}\text{O}$ values ranging from -10 to -11‰ (Turgeon, 2001), suggesting warmer average temperatures over OCNM during the early versus the late Holocene. A similar contrast between early and late Holocene SSTs occurred off the Oregon coast (Mix et al., 1999; Barron et al., 2003).

Additionally, there is significant centennial-scale variability within our early Holocene $\delta^{18}\text{O}$ record that indicates significant temperature changes (Fig. 4c). In particular, we note a warming event at 11,000 yr ago that is comparable in $\delta^{18}\text{O}$ amplitude to temperature change estimated for the YD. As a preliminary analysis of the centennial variability for our record, we used a ten-point running mean smoother to remove millennial-scale variability and evaluated the residuals of that smoothing in terms of the strength of centennial-scale modes. Autocorrelation analysis yielded 95% significance correlations over the lags 140–250 yr. Spectral analysis of the record showed a narrow-band signal having a period of 190 yr. Because of the brevity of our record (4000 yr) relative to such bicentennial-scale variability, potential errors associated with detrending of millennial-scale variations, possible changes in accumulation rate and coarse sampling intervals, these time series analyses are susceptible to sampling bias and should be considered preliminary.

Our OCNM $\delta^{13}\text{C}$ record shows a relatively steady progression from values $> -2\text{‰}$ 13,300 yr ago to early Holocene values that average -7‰ , with a limited expression of a YD signal (Fig. 4d). A pollen record from Bolan Lake, Oregon, 10 km southwest of OCNM, indicates that C_3 plants have dominated the vegetation type in this region over the last 14,000 yr (Briles, 2003), suggesting that the trend towards lighter $\delta^{13}\text{C}$ values in our record cannot be attributed to a transition from C_4 to C_3 plants. Because $\delta^{13}\text{C}$ values $< -6\text{‰}$ are expected for a carbonate system dominated by C_3 plants (Baker et al., 1997), we interpret the trend of decreasing $\delta^{13}\text{C}$ values to record an increasing contribution from soil respiration rates relative to contributions from atmospheric CO_2 and carbonate bedrock ($+1.7\text{‰}$ at OCNM; Turgeon, 2001). The Bolan Lake pollen record, for example, suggests that conifer forests migrated upslope after 14,500 yr ago, replacing sparse subalpine parkland vegetation near upper treeline (Briles, 2003). A forest composition similar to present only became established after 13,000 yr ago. The subsequent decrease in OCNM $\delta^{13}\text{C}$ values may thus reflect some combination of an

increase in biomass, an increase in moisture to enhance decay of organic matter and the relatively long time for buildup of organic matter in soils. The late Holocene (4000–2000 yr ago) OCNM $\delta^{13}\text{C}$ record (Turgeon, 2001) has similar average values (-7 to -8‰) as our early Holocene $\delta^{13}\text{C}$ record, suggesting that the modern soil CO_2 reservoir was established by $\sim 11,000$ yr ago (Fig. 3).

Century-scale variations in $\delta^{13}\text{C}$ of 1–2‰ occur throughout the early Holocene, although there is no apparent correlation with the $\delta^{18}\text{O}$ record (Fig. 4). Such short-term variations may reflect variations in soil moisture and attendant rates of organic matter decay.

Conclusions

Proxy records indicate that YD cooling in the North Atlantic region was induced by a reduction in the Atlantic meridional overturning (AMO) and attendant heat transport (Hughen et al., 2000; McManus et al., 2004). Simulations with coupled atmosphere–ocean general circulation models suggest that zonal transmission of Atlantic thermal anomalies through the atmospheric circulation causes cooling over the entire extratropics of the Northern Hemisphere (Manabe and Stouffer, 1988; Mikolajewicz et al., 1997; Vellinga and Wood, 2002). The synchronicity of the YD signal in three widely separated areas of the Northern Hemisphere (GISP2, Hulu Cave, OCNM) (Fig. 4) supports this mechanism. In particular, relatively high $\delta^{18}\text{O}$ values from Hulu Cave record weakening of the East Asian summer monsoon in response to cooling over Siberia (Wang et al., 2001), whereas the relatively low OCNM $\delta^{18}\text{O}$ values record cooling of the North Pacific associated with enhanced cold-air advection from Siberia, although decreased upwelling along the North American margin may have moderated this response (Mikolajewicz et al., 1997; Mix et al., 1999).

We note that the magnitude of northeast Pacific cooling indicated by SST reconstructions (Barron et al., 2003) is substantially larger than temperature changes simulated by these models. In part, this disagreement may reflect the modern boundary conditions used in the models, whereas the remnant Northern Hemisphere ice sheets and lower atmospheric greenhouse gas concentrations during the YD contributed to additional cooling. Feedbacks not well represented in the models, such as changing oceanic heat transport driven by the balance of surface and subsurface ocean flows, or regional expansion of snow cover in unresolved mountainous terrain, may also have contributed to a larger response.

Acknowledgments

We thank John Dodge for providing the speleothem to Oregon State University for study and John Roth of the

Oregon Caves National Monument for his support. Comments from two anonymous reviewers significantly improved the paper.

References

- Adkins, J.F., McIntyre, K., Schrag, D.P., 2002. The salinity, temperature, and $\delta^{18}\text{O}$ of the glacial deep ocean. *Science* 298, 1769–1773.
- Alley, R.B., Marotzke, J., Nordhaus, W.D., Overpeck, J.T., Peteet, D.M., Pielke Jr., R.A., Pierrehumbert, R.T., Rhines, P.B., Stocker, T.F., Talley, L.D., Wallace, J.M., 2003. Abrupt climate change. *Science* 299, 2005–2010.
- Baker, A., Ito, E., Smart, P.L., McEwan, R.G., 1997. Elevated and variable values of ^{13}C in speleothems in a British cave system. *Chemical Geology* 136, 263–270.
- Barron, J.A., Heusser, L., Herbert, T., Lyle, M., 2003. High-resolution climatic evolution of coastal northern California during the past 16,000 years. *Paleoceanography* 18, 1020.
- Bartlein, P.J., Anderson, K.H., Anderson, P.M., Edwards, M.E., Mock, C.J., Thompson, R.S., Webb, R.S., Webb III, T., Whitlock, C., 1998. Paleoclimate simulations for North America over the past 21,000 years: features of the simulated climate and comparisons with paleoenvironmental data. *Quaternary Science Reviews* 17, 549–585.
- Briles, C.E., 2003. Postglacial vegetation and fire history near Bolan Lake in the Northern Siskiyou Mountains of Oregon. Master's Thesis. Department of Geography, University of Oregon. 148 pp.
- Cerling, T.E., 1984. The stable isotopic composition of modern soil carbonate and its relationship to climate. *Earth and Planetary Science Letters* 71, 229–240.
- Cerling, T.E., Quade, J., Wang, Y., Bowman, J.R., 1989. Carbon isotopes in soils and palaeosols as ecology and palaeoecology indicators. *Nature* 341, 138–139.
- Cheng, H., Edwards, R.L., Hoff, J., Gallup, C.D., Richards, D.A., Asmerom, Y., 2000. The half-lives of uranium-234 and thorium-230. *Chemical Geology* 169, 17–33.
- Clark, P.U., Pisias, N.G., Stocker, T.F., Weaver, A.J., 2002. The role of the thermohaline circulation in abrupt climate change. *Nature* 415, 863–869.
- Dansgaard, W., 1964. Stable isotopes in precipitation. *Tellus* 16, 436–468.
- Dorale, J.A., Edwards, R.L., Alexander, E.C., Shen, C.-C., Richards, D.A., Cheng, H., 2004. Uranium-series dating of speleothems: current techniques, limits, and applications. In: Sasowski, I.D., Mylroie, J. (Eds.), *Studies of Cave Sediments*. Kluwer Academic/Plenum, New York.
- Edwards, R.L., Chen, J.H., Wasserburg, G.J., 1987. U-238, U-234, Th-230, Th-232 systematics and the precise measurement of time over the past 500,000 years. *Earth and Planetary Science Letters* 81, 175–192.
- Eppstein, S., Mayeda, T.K., 1953. Variations of the $^{18}\text{O}/^{16}\text{O}$ ratio in natural waters. *Geochimica et Cosmochimica Acta* 4, 213.
- Fantidis, J., Ehler, D.H., 1970. Variations of the carbon and oxygen isotopic composition in stalagmites and stalactites: evidence of non-equilibrium isotopic fractionation. *Earth and Planetary Science Letters* 10, 136–144.
- Fleming, K., Johnston, P., Zwart, D., Yokoyama, Y., Lambeck, K., Chappell, J., 1998. Refining the eustatic sea-level curve since the last glacial maximum using far- and intermediate-field sites. *Earth and Planetary Science Letters* 163, 327–342.
- Genty, D., Blamart, D., Ouahdi, R., Gilmour, M., Baker, A., Jouzel, J., Van-Exter, S., 2003. Precise dating of Dansgaard–Oeschger climate oscillations in western Europe from stalagmite data. *Nature* 421, 833–837.
- Groote, P.M., Stuiver, M., White, J.W.C., Johnsen, S.J., Jouzel, J., 1993. Comparison of oxygen isotope records from the GISP2 and GRIP Greenland ice cores. *Nature* 366, 552–554.
- Hendy, C.H., 1971. The isotopic geochemistry of speleothems-I. The calculation of the effects of different modes of formation on the isotopic composition of speleothems and their applicability as palaeoclimatic indicators. *Geochimica et Cosmochimica Acta* 35, 801–824.
- Hughen, K.A., Southon, J.R., Lehman, S.J., Overpeck, J.T., 2000. Synchronous radiocarbon and climate shifts during the last deglaciation. *Science* 290, 1951–1954.
- Kienast, S., McKay, J.L., 2001. Sea surface temperatures in the subarctic northeast Pacific reflect millennial-scale climate oscillations during the last 16 kyr. *Geophysical Research Letters* 28, 1563–1566.
- Manabe, S., Stouffer, R.J., 1988. Two stable equilibria of a coupled ocean–atmosphere model. *Journal of Climate* 1, 841–866.
- Mantua, N.J., Hare, S.R., Zhang, Y., Wallace, J.M., Francis, R.C., 1997. A Pacific interdecadal climate oscillation with impacts on salmon production. *Bulletin of the American Meteorological Society* 78, 1069–1079.
- McManus, J.F., Francois, R., Gherardi, J.-M., Keigwin, L.D., Brown-Leger, S., 2004. Collapse and rapid resumption of Atlantic meridional circulation linked to deglacial climate changes. *Nature* 428, 834–837.
- Mikolajewicz, U., Crowley, T.J., Schiller, A., Voss, R., 1997. Modelling teleconnections between the North Atlantic and North Pacific during the Younger Dryas. *Nature* 387, 384–387.
- Mix, A.C., Lund, D.C., Pisias, N.G., Boden, P., Bornmalm, L., Lyle, M., Pike, J., 1999. Rapid climate oscillations in the Northeast Pacific during the last deglaciation reflect northern and southern hemisphere sources. In: Clark, P.U., Webb, R.S., Keigwin, L.D. (Eds.), *Mechanisms of Global Climate Change at Millennial Time Scales*; Geophysical Monograph 112. American Geophysical Union, pp. 127–148.
- Mortyn, P.G., Thunell, R.C., Anderson, D.M., Stott, L.D., Le, J., 1996. Sea surface temperature changes in the southern California borderlands during the last glacial-interglacial cycle. *Paleoceanography* 11, 415–430.
- NIST, 1992a. National Institute of Standards and Technology Report of Investigation, Reference Materials 8543–8546. National Institute of Standards and Technology, United States Department of Commerce, Gaithersburg, Maryland, 2 pp.
- NIST, 1992b. National Institute of Standards and Technology Report of Investigation, Reference Materials 8535–8537. National Institute of Standards and Technology, United States Department of Commerce, Gaithersburg, Maryland, 2 pp.
- O'Neill, J.R., Clayton, R.N., Mayeda, T.K., 1969. Oxygen isotope fractionation in divalent metal carbonates. *Journal of Chemical Physics* 51, 5547–5558.
- Ortiz, J.D., Mix, A.C., Hostetler, S., Kashgarian, M., 1997. The California current of the last glacial maximum: reconstruction at 42°N based on multiple proxies. *Paleoceanography* 12, 191–206.
- Rozanski, R., Araguas-Araguas, L., Gonfiantini, R., 1993. Isotopic patterns in modern global precipitation. In: Swart, P., McKenzie, J.A., Lohman, K.C. (Eds.), *Continental Indicators of Climate*: American Geophysical Union Monograph, vol. 78, pp. 1–36.
- Schmidt, G.A., Bigg, G.R., Rohling, E.R., 1999. Global seawater oxygen-18 database. <http://www.giss.nasa.gov/data/s18data/>.
- Shen, C.-C., Edwards, R.L., Cheng, H., Dorale, J.A., Thomas, R.B., Moran, S.B., Weinstein, S., Edmonds, H.N., 2002. Uranium and thorium isotopic and concentration measurements by magnetic sector inductively coupled plasma mass spectrometry. *Chemical Geology* 185, 165–178.
- Stuiver, M., Grootes, P.M., 2000. GISP2 oxygen isotope ratios. *Quaternary Research* 53, 277–284.
- Turgeon, S.C., 2001. Petrography and discontinuities, growth rates and stable isotopes of speleothems as indicators of paleoclimates from Oregon Caves National Monument, southwestern Oregon, USA. PhD dissertation. Department of Geography, Carleton University. 213 pp.

- Vellinga, M., Wood, R.A., 2002. Global climatic impacts of a collapse of the Atlantic thermohaline circulation. *Climatic Change* 54, 251–267.
- Voelker, A.H.L., et al., 2002. Global distribution of centennial-scale records for marine isotope stage (MIS) 3: a database. *Quaternary Science Reviews* 21, 1185–1214.
- Wang, Y.J., Cheng, H., Edwards, R.L., An, Z.S., Wu, J.Y., Shen, C.C., Dorale, J.A., 2001. A high-resolution absolute-dated late Pleistocene monsoon record from Hulu Cave, China. *Science* 294, 2345–2348.
- Yuan, D.X., Cheng, H., Edwards, R.L., Dykoski, C., Kelly, M.J., Zhang, M.L., Qing, J.M., Lin, Y.S., Wang, Y.G., Dorale, J.A., An, Z.S., Cai, Y.J., 2004. Timing, duration, and transitions of the Last Interglacial Asian Monsoon. *Science* 304, 575–578.